Binding site models of friction due to the formation and rupture of bonds: State-function formalism, force-velocity relations, response to slip velocity transients, and slip stability

Manoj Srinivasan*
Mechanical Engineering, Ohio State University, Columbus, Ohio 43210, USA
and Mechanical and Aerospace Engineering, Princeton University, Princeton, New Jersey 08544, USA

Sam Walcott†
Department of Mechanical Engineering, Johns Hopkins University, Baltimore, Maryland 21218, USA
(Received 2 December 2008; revised manuscript received 6 July 2009; published 26 October 2009)

We present a model describing friction due to the thermally activated formation and rupture of molecular bonds between two surfaces, with long molecules on one surface attaching to discrete or continuous binding sites on the other. The physical assumptions underlying this model are formalized using a continuum approximation resulting in a class of master-equation-like partial differential equations that is a generalization of a friction model due to Persson [Phys. Rev. B **51**, 13568 (1995)] and is identical to the equations used to describe muscle contraction, first proposed by A. F. Huxley. We examine the properties of this friction model in the continuous binding site limit noting that this model is capable of producing both monotonically increasing and an increasing-decreasing force dependence on slip velocity. When monotonically increasing, the force dependence on velocity is (asymptotically) logarithmic. The model produces a transient increase in friction in response to a sudden velocity increase, whether or not the steady-state friction force is a decreasing or increasing function of steady slip velocity. The model also exhibits both stable steady slip and stick-slip-like oscillatory behavior, in the presence of compliance in the loading machine, even when the steady-state friction force is a decreasing function of steady-state slip velocity.

DOI: 10.1103/PhysRevE.80.046124 PACS number(s): 81.40.Pq

I. INTRODUCTION

A substantial literature exists within the physics and mechanics communities attempting to construct theories and models that capture the molecular, or otherwise microscopic, origins of friction between solid surfaces (e.g., [1–30]). While these models have had various degrees of success, there seems to be a consensus that a relatively complete and satisfactory understanding of the molecular and mesoscopic origins of friction is still open [31].

In this paper, we describe a class of microscopic friction models that model friction as arising from the thermally activated formation and rupture of springy molecular bonds between two rigid surfaces. A number of friction models have previously been proposed in the friction literature invoking similar physical mechanisms but somewhat different in detail. To clearly distinguish our friction model, we now review these prior friction models briefly and comment on our models' relation to these models.

First, there exists a large class of earthquake models consisting of an elastically coupled chain of masses interacting with a planar rough surface via some macroscopic friction model. Most models in this class (e.g., [3,32–35]) are either modifications or generalizations of the model due to Burridge and Knopoff [36]. These earthquake models are superficially similar to the models described in this paper (due to the presence of an ensemble of spring-mass systems), but there are important differences. The intent of these earthquake models is not necessarily to understand the microscopic origins of friction, but to infer the consequences of specific assumed friction models to earthquake dynamics, or more generally, the frictional properties at larger spatial scales given the frictional properties at smaller (but still much larger than molecular) spatial scales. Also, the friction laws used in these earthquake models do not have the chemical-reaction-like features that the models described here possess. Somewhat related to the earthquake models are models of asperities (modeled again as masses on springs) on opposing surfaces, making and breaking contact—the asperities could be modeled as breaking contact at a specific strain or at a broad range of strains, with a particular probability distribution (e.g., [37]).

Persson [19] considers the frictional interaction between an elastic block sliding on a surface with a thin lubrication film of molecular thickness. He considers the lubrication layer to not be a smooth fluid state but containing pinned stress domains that fluidize and refreeze while sliding. He models these stress domains as a chain of masses connected by springs and formulates an integropartial differential equation that we show here to be a special case of the Lacker-Peskin continuous binding site model presented in this paper—we will expand on the relation between the two models later in this paper. In this sense, the models we describe in this paper can be considered as generalizations of that due to Persson [19].

Filippov *et al.* [7] recently presented a model in which friction arose from the thermally activated formation and rupture of (an ensemble of) molecular bonds. The physical assumptions in their model are also most similar to the so-called Lasker-Peskin model presented here with minor dif-

*srinivasan.88@osu.edu; http://movement.osu.edu
†samwalcott@gmail.com

ferences. Their model of bond rupture is essentially identical to that used here, but their model for bond formation is different from that used here (it is independent of bond length, but dependent on the "age" of the contact, while our models assume the converse). While Filippov *et al.* present only the simulation results from their model, our continuum approximation of the physical assumptions enables us to obtain some analytical results. Given the close relatedness of the models, it is possible that our formalism could be adapted to better understand the Filippov *et al.* model.

Another closely related class of friction models are modifications of that introduced by Tomlinson [24], most recently used to explain the frictional interaction between the tip of an atomic force microscope or a friction force microscope (e.g., [10,38–41]) and an atomically flat surface. Tomlinson-like models usually consist of a mass on a spring, possibly thermally activated, interacting with a periodic potential imposed by a periodic lattice of surface atoms. One generalization of the Tomlinson model is the so-called Frenkel-Kontorova-Tomlinson (FKT) model in which an interacting chain of masses connected by springs on one surface interacts with a periodic potential imposed by the other surface [25,26,40]. An FKT-like model was recently used in the modeling of the adhesive and frictional interaction between a biological cell and a substrate [42]. The models in our paper might be thought of as being a different and somewhat stylized generalization of the Tomlinson models, first replacing the "periodic potential" by a sequence of "discrete binding sites" corresponding to the energy wells, and then possibly taking the limit of arbitrarily closely spaced (Lacker-Peskin model here) or sparsely spaced binding sites (Huxley model here). The physical assumptions underlying the models here are also closely related to the theory of elastomeric friction due to Schallamach [43], who only considered steady-state properties; but see [30] for the derivation of a dynamical PDE describing such friction, different from those derived here.

Finally, we note that our models are only-slightly-modified versions of classic molecular models used to describe the function of skeletal muscles [44–52]. Skeletal muscles consist of a regular lattice of parallel filaments of two types, referred to as thick and thin filaments, composed largely of actin, myosin, and other long-chain protein molecules. Muscles shorten by the relative sliding of these parallel filaments and convert chemical energy into force and/or mechanical work by the repeated binding and unbinding of the myosin heads on the thick filament with the actin binding sites on the thin filaments. This "sliding filament" description of muscle contraction was proposed in back-to-back *Nature* papers in 1954, co-authored independently by two unrelated Huxley's [53,54]. In 1957, A. F. Huxley organized these largely experimental observations into a simple mathematical model resulting in a partial differential equation (PDE) describing the mechanics of muscle contraction [47]. This PDE and generalizations thereof remain the current rational foundation for the understanding of muscle mechanics at the molecular level. The friction model PDEs we derive here are identical to the muscle model PDEs—so we sometimes refer to them here using their muscle mechanician progenitors (Huxley PDE or Lacker-Peskin PDE). But we must emphasize that the binding sites-based friction models described here stand on their own merits motivated independently by basic physical mechanisms that are thought to be relevant to friction and are of interest to friction mechanicians both because the phenomenology they are capable of and because of their generalizing relation to some prior friction models.

We now briefly describe the organization of the paper. In Sec. II, we describe our molecular friction model in two parts. In Sec. II A we introduce a general binding site model in which friction is produced by an ensemble of masses on springs on one surface attaching to a series of binding sites on the opposing surface. This section mostly follows the corresponding muscle exposition in [48]. Then, we specialize this general binding site model taking the limit of dense binding sites (the Lacker-Peskin model in Sec. II A 1) and the limit of sparse binding sites (the Huxley model in Sec. II A 2). In the main body of the paper, we focus on the Lacker-Peskin continuous binding site model under a few different conditions, while Appendix A provides analogous results for the Huxley sparse binding site limit. In Sec. II B, using reaction rate theory, we briefly derive plausible models for bond formation and rupture that we use for the rest of the paper. Coupling these models of bond formation and rupture to the binding sites models, we perform a variety of analytical and numerical calculations described in Sec. III. First, in Sec. III A, we derive expressions for the steady-state force-velocity relations for these models and obtain some asymptotic expressions. Then, in Sec. III B, we obtain the response of the friction force in these models to discontinuous changes in slip velocity and we make a prediction that there will be an overshoot in the friction force before the obtaining of steady state. Then, in Sec. III C, we show that the Lacker-Peskin friction model can exhibit both stable steady slip (despite the steady-state friction force decreasing with slip speed) and oscillatory slip (with unstable steady slip) depending on the stiffness of the loading machine. Finally, in Sec. IV, we briefly compare our model to the empirically based state-variable laws of Dieterich and Ruina. We finish this section with a discussion of direct applications of our model to biological friction.

II. MODEL

Our molecular friction model consists of two large rigid surfaces capable of sliding relative to each other. Long-chain molecules on one surface interact with binding sites on the other surface. In this section, we write a mathematical model of this system in two steps. First, without specifying the details of the molecular interactions of the long-chain molecules, we obtain a partial differential equation model for long-chain molecules interacting with two sliding surfaces. Then, invoking Kramers' reaction rate theory, we derive a plausible mathematical description for the chemical interactions of the long-chain molecules and their binding sites.

A. General binding site model

The general model [Fig. 1(a)] consists of two blocks, which are rigid, very long, with their interacting surfaces

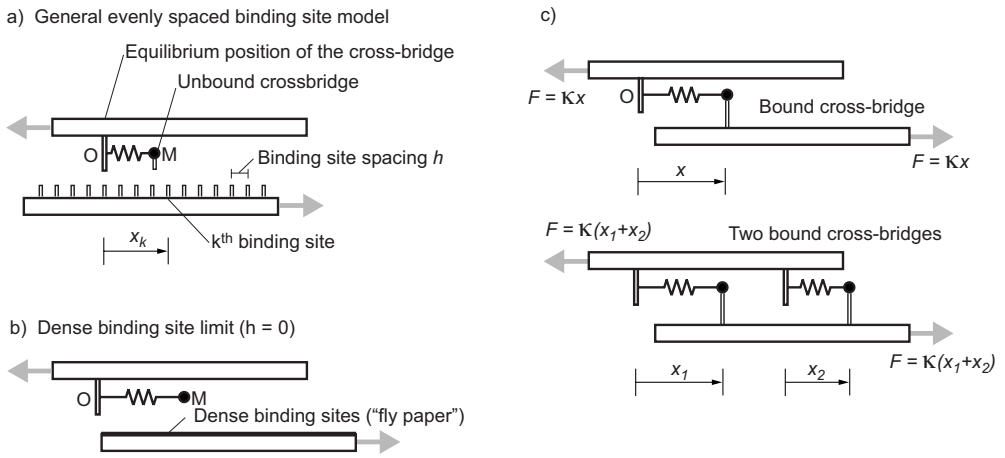

FIG. 1. (a) Model with evenly spaced binding sites, with spacing h, small enough that any given cross-bridge on the top surface can interact with more than one binding site on the bottom surface. (b) When $h \to 0$, the cross-bridge can attach to any point on the bottom surface; this is the dense or continuous binding sites limit giving the Lacker-Peskin equation. (c) A single cross-bridge attached to its binding site implies a tensional force $F=\kappa x$ in the filaments. When multiple cross-bridges are attached, the force transmitted by them add (the cross-bridges are in parallel).

parallel to each other, and attached to the external world at their extremes. One of the surfaces has numerous springy elements called "cross-bridges" (long-chain molecules), which can attach to corresponding binding sites on the opposing surface.

For simplicity, we assume that the cross-bridges are always in one of two states: bound (B) or unbound (U). This derivation is readily generalized to include multiple states [55]. Figure 1(a) shows a single cross-bridge capable of binding to any of the binding sites shown. The binding sites are indexed by integers. The kth binding site is a distance x_k from the base O of the cross-bridge with $k \in \{\ldots,-2,\ -1,\ 0,\ 1,\ 2,\ldots\}$. The reaction network for this system is such that the cross-bridges can bind to any of the binding sites from the unbound state but are unable to directly go from being bound to one binding site to another. The binding and unbinding of an ensemble of identical cross-bridges with the kth binding site are governed by reaction rates that are dependent on x_k:

$$\mathrm{U} \underset{g(x_k)}{\overset{f(x_k)}{\rightleftharpoons}} \mathrm{B}, \tag{1}$$

where $g(x_k)$ is the unbinding rate function and $f(x_k)$ is the binding rate function. The rate functions g and f are assumed to be the same for all the binding sites.

If none of the cross-bridges are attached to the binding sites, the total (time-averaged) friction force F between the two surfaces is zero. The springy cross-bridges, when attached to their binding sites, transmit a force that is a monotonic function of the strain x, for instance, κx [Fig. 1(c)], where κ is a spring constant. The total friction force F is equal to the sum of the forces due to all the bound cross-bridges, as shown in Fig. 1(c) for two bound cross-bridges.

Now consider an ensemble of M cross-bridges, all at the same position relative to the grid of binding sites. The two surfaces are at rest relative to each other. We define $n_k(t)$ to be the fraction of the M cross-bridges that are bound to the kth binding site. The rate of change of this fraction $dn_k(t)/dt$ is given by the sum of the two following terms. (1) binding rate: a binding rate function $f(x_k)$ times the fraction unbound $(1-\Sigma_k n_k)$; (2) unbinding rate: an unbinding rate function $g(x_k)$ times the fraction bound to the kth binding site n_k,

$$\frac{dn_k}{dt} = \left(1 - \sum_k n_k\right) f(x_k) - n_k g(x_k). \tag{2}$$

We now examine this equation under two extreme limits of h and generalize it to when the two surfaces slide past each other.

1. Continuous (dense) binding sites: The Lacker-Peskin model

Lacker and Peskin [49–52], in the context of muscles, considered the limit of very dense binding sites, letting the spacing $h \to 0$, so that the position of the cross-bridges relative to the grid becomes irrelevant. This lets us set $x_0=0$, without loss of generality, so that $x_k=x_0+kh=kh$. Then, Eq. (2) becomes

$$\frac{dn_k}{dt} = \left(1 - \sum_k n_k\right) f(kh) - n_k g(kh).$$

Dividing through by h, we obtain

$$\frac{d(n_k/h)}{dt} = \left[1 - h\sum_k (n_k/h)\right]\frac{f(kh)}{h} - \frac{n_k g(kh)}{h}. \tag{3}$$

Now, we define a smooth function $n(x,t)$, so that its discretized version on the grid $x_k=kh$ is given by $n_k(t)/h$; that is, $n(kh,t)=n_k(t)/h$. Then, defining $f_p(x)=f(x)/h$ and $g_p(x)=g(x)$, we can treat Eq. (3) as a spatially discretized version of the partial differential equation:

$$\frac{\partial n(x,t)}{\partial t} = \left[1 - \int_{-\infty}^{\infty} n(x,t)dx\right] f_p(x) - n(x,t)g_p(x).$$

If the bottom surface was moving to the right relative to the top surface, at velocity $v(t)$, the PDE is modified by a convective term, giving

$$\frac{\partial n}{\partial t} + v\frac{\partial n}{\partial x} = \left(1 - \int_{-\infty}^{\infty} n dx\right) f_p(x) - n g_p(x), \tag{4}$$

which we call the Lacker-Peskin PDE for the continuous binding site limit [49–52]. If M is the total number of cross-bridges, bound or unbound, the total force F produced by the ensemble of bound cross-bridges is given by

$$F(t) = M\int_{-\infty}^{\infty} \kappa x n(x,t)dx. \tag{5}$$

For the continuous binding limit, the quantity x has meaning only for a bound cross-bridge (and meaningless when the cross-bridge is unbound). Thus, the function $n(x,t)$ has the following meaning: the fraction of all the total cross-bridges that find themselves bound with a strain between x and $x+\Delta x$ is given by $n(x,t)\Delta x$ to first order.

Note that the rate function $f_p(x)$ was obtained as the limit $f(x)/h$. We can interpret this one of two ways. First, if we imagine the Lacker-Peskin PDE as indeed the limit of $h \to 0$, then to get a finite $f_p(x)$, we must scale $f(x)$ with h. That is, each binding site must become weaker as the binding sites become denser, so that the "attraction" over unit length remains bounded. Alternatively, consistent with the derivation above, we can imagine the Lacker-Peskin PDE as a continuum approximation for small h. In this case, the limit $h \to 0$ is not taken and we can simply set $f_p(x) = f(x)/h$. We prefer the latter perspective.

In the main body of this paper, we will mostly consider the Lacker-Peskin continuous binding sites model, as it seems more appropriate for the description of the potential energy minima induced by an atomic lattice. Also, we show in Appendix B that the Persson friction model [19] is a special case of the Lacker-Peskin model corresponding to the case when the cross-bridge that gets unbound gets immediately bound with $x=0$.

2. Sparse binding sites: The Huxley model

The other limit of potential interest is to assume that the binding sites are so sparse—h is so great—that the cross-bridge can interact with only one of the binding sites, say, with $k=0$. Then, in Eq. (2), we have $n_k \equiv 0$ for $k \neq 0$. We have only one equation left:

$$\frac{dn_0}{dt} = (1 - n_0)f(x_0) - n_0 g(x_0). \tag{6}$$

If the bottom block moves to the right relative to the top block, with a relative velocity $v(t)$, the above equation would be modified by a convective transport term giving the following PDE:

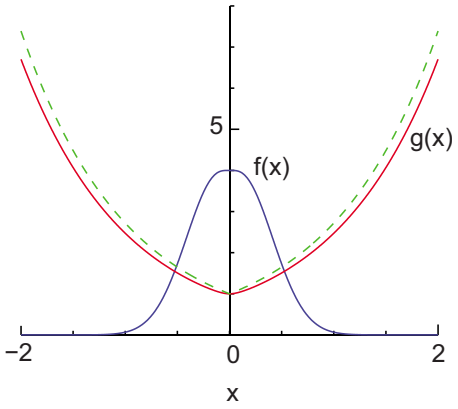

FIG. 2. (Color online) The smooth rate functions for binding and unbinding, $f(x)$ and $g(x)$, used in this paper [Eqs. (10) and (11)]. The dotted line is the simpler approximation to $g(x)$ from Eq. (12).

$$\frac{\partial n_h}{\partial t} + v(t)\frac{\partial n_h}{\partial x} = (1 - n_h)f(x) - n_h g(x), \tag{7}$$

where we have replaced x_0 with x and n_0 with n_h (the subscript h stands for Huxley). In this equation, $n_h(x,t)$ is the probability that a given cross-bridge, whose base is at a distance x from the single binding site it can interact with, is bound to this binding site. Equation (7) is the classic PDE that Huxley [47] derived for describing the mechanics of muscle contraction and force production. So we call this limit the Huxley model, or alternatively, the sparse binding sites model. The total force due to all the bound cross-bridges is given by integrating over x:

$$F(t) = \rho\int_{-\infty}^{\infty} \kappa x n_h(x,t)dt, \tag{8}$$

where ρ is the total number of cross-bridges, bound or unbound, per unit x, assumed to be a constant [47]. Note, therefore, that this $n_h(x,t)$ has a different interpretation from the $n(x,t)$ for the Lacker-Peskin dense binding site limit.

B. Rate functions for binding and unbinding

For a cross-bridge bound with a strain x, it seems intuitive that the propensity to unbind would increase with $|x|$. Conversely, for an unbound cross-bridge, the propensity to bind would decrease with $|x|$. We now derive rate functions (shown in Fig. 2) consistent with this intuition. A less rigorous version of this derivation appears in the supplementary material of [56].

To derive the rate functions, we use the high-damping limit of Langer's [57] reaction rate theory expressions for the escape of Brownian particles from potential wells in many dimensions, a generalization of Kramers' theory [58]. Say $V(\mathbf{z})$ is the potential energy function and $E(\mathbf{z},\dot{\mathbf{z}})$ is the total energy function. The potential energy function has minima at points B and U and a saddle point S between them. Say $\mathbf{H}_U$ and $\mathbf{H}_S$ are the Hessians of the energy function $E(\mathbf{z},\dot{\mathbf{z}})$ with respect to $[\mathbf{z};\dot{\mathbf{z}}]$ at U and S, and λ^+ is the dominant growth rate near the saddle. Then, in the intermediate to high damp-

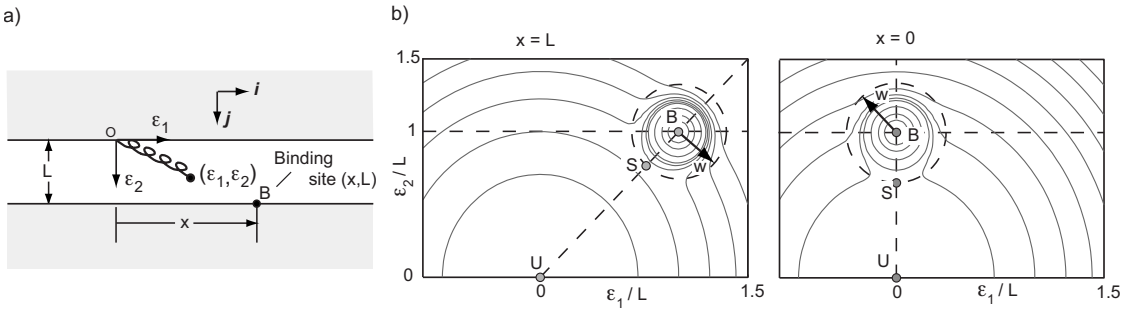

FIG. 3. (a) A two-dimensional model for binding. The top surface has a springy cross-bridge (point mass attached to a spring) that can "bind" to a binding site B on the bottom surface at a horizontal distance x from the base of the spring. Two surfaces are separated by a small distance L. The coordinates of the point mass on the cross-bridge is $(\varepsilon_1,\varepsilon_2)$. (b) The contours of the potential energy for the mechanical model (units of k_bT) as a function of the two spatial dimensions ε_1 and ε_2. The bound (B), unbound (U), and transition (S) state are shown as gray dots. Two different values of x, the spacing between B and U along ε_1, are shown: $x=L$ and $x=0$.

ing limit, the rate constant k_{escape} of escape from the potential energy minimum U is given, approximately, by

$$k_{escape} = \frac{\lambda^+}{2\pi}\sqrt{\frac{\det(\mathbf{H}_U)}{|\det(\mathbf{H}_S)|}}e^{-(V_S-V_U)/k_bT}, \tag{9}$$

where k_b is the Boltzmann constant and T is the temperature, as conventional (see [59] for this formula).

We use the above expression [Eq. (9)] in the context of a simple *two-dimensional* model for cross-bridge binding shown in Fig. 3(a). Consider a point mass moving in 2D attached to a linear, zero-length spring with stiffness κ [this is the "cross-bridge;" see Fig. 3(a)]. The base of the spring is fixed in space attached to a horizontal surface. Some distance L away, there is another large flat surface with a binding site at a distance x from the base of the spring. The 2D position of the point mass relative to the base of the spring is given by the vector $\boldsymbol{\varepsilon}=\varepsilon_1\boldsymbol{i}+\varepsilon_2\boldsymbol{j}$.

The zero-length spring creates a quadratic potential V_s. We model the binding site B as inducing a localized additive potential well $V_{bs}(\boldsymbol{\varepsilon})$ that is narrow and deep, so that the total potential energy $V=V_s+V_{bs}$. The potential energy contours are shown in Fig. 3(b) for two different x values. The total energy function is $E=m(\dot{\varepsilon}_1^2+\dot{\varepsilon}_2^2)/2+V(\boldsymbol{\varepsilon})$.

The system can be in one of two states: "bound" B (i.e., in the basin of attraction of the binding site) or "unbound" U (i.e., in the basin of attraction of the spring's potential well). The critical point on the potential energy surface associated with the unbound state U is approximately $\boldsymbol{\varepsilon}\approx\mathbf{0}$. Similarly, $\boldsymbol{\varepsilon}\approx\boldsymbol{\varepsilon}_0$ will be the critical point associated with the bound state B, where $\boldsymbol{\varepsilon}_0$ is the location of the binding site.

For a circular potential well V_{bs}, the three critical points of the potential energy surface (the bound, unbound, and transition states) must lie on a straight line by symmetry. Noting that the distance w [see Fig. 3(b)] from the bound state to the transition state, the saddle point S, is approximately constant with x, the position $\boldsymbol{\varepsilon}^S=\varepsilon_1^S(x)\boldsymbol{i}+\varepsilon_2^S(x)\boldsymbol{j}$ of the saddle point is

$$\varepsilon_1^S(x) = x - \frac{wx}{\sqrt{x^2+L^2}} \quad \text{and} \quad \varepsilon_2^S(x) = L - \frac{wL}{\sqrt{x^2+L^2}}.$$

Using these approximations, we may write the potential V_S at the transition state as

$$V_S \approx V_{S0} - \frac{\kappa}{2}(L-w)^2 + \frac{\kappa}{2}\left[\left(x-\frac{wx}{\sqrt{L^2+x^2}}\right)^2 + \left(L-\frac{wL}{\sqrt{L^2+x^2}}\right)^2\right],$$

where V_{S0} is the potential energy of the transition state when $x=0$.

At the unbound state U, the determinant of the Hessian of the energy is given by $\det(\mathbf{H}_U)=m^2\kappa^2$. At the saddle point S, the determinant of the Hessian of the energy is given by $\det(\mathbf{H}_S)=m^2\lambda_1\lambda_2$, where $\lambda_1>0$ and $\lambda_2<0$ are the principal curvatures of the potential energy at S. If the damping coefficient is γ, writing the linearized dynamics equations for $[\boldsymbol{\varepsilon}\dot{\boldsymbol{\varepsilon}}]$ near the saddle point S, it can be shown that the dominant growth rate near the saddle S is $\lambda^+=(-1+\sqrt{1+4m|\lambda_2|/\gamma})\gamma/2m$, which is well approximated by $|\lambda_2|/\gamma$ for large damping coefficient γ.

Assembling all the pieces in Eq. (9), using $V_U=0$, and neglecting the x dependence of λ_i, we can show that

$$f(x) = f_0\exp[-bx^2 + a(\sqrt{c^2+x^2}-c)], \tag{10}$$

with $b=\kappa/2k_bT$, $a=\kappa w/k_bT$, and $c=L$; and f_0 is the reaction rate when $x=0$, i.e., the maximum reaction rate.

Similarly, we may write an expression for the unbinding rate constant g:

$$g(x) = g_0\exp[a(\sqrt{c^2+x^2}-c)], \tag{11}$$

where $g(0)=g_0$ is the minimum unbinding rate and $a=\kappa w/k_bT$ and $c=L$ as before.

Figure 2 shows the rate functions for $a=1$, $b=5$, $c=0.1$, $f_0=4$, and $g_0=1$. We use these parameter values throughout this paper. These parameters are not special in any way and the qualitative behavior described here generalizes to other parameter values.

For the Lacker-Peskin model, we use rate functions of the same form except scaling the binding rate function by the appropriate binding site spacing. That is, we use $f_p(x)=f(x)/h$ and $g_p(x)=g(x)$, where h is the binding site spacing. We use $h=0.1$ in the calculations corresponding to the Lacker-Peskin model.

We may simplify these expressions for the rate functions if we take the limit as $\kappa \to \infty$; i.e., the molecular spring becomes very stiff. However, in order to have the chemical reactions occur at a non-negligible rate, we must also adjust w and L letting them become very small. Recall, w is the effective radius of the binding well and depends on the details of the binding well. Therefore, we may pick w and L to scale as $1/\kappa$, $w = c_w k_b T/(\ell\kappa)$ and $L = c_L k_b T/(\ell\kappa)$, where c_w and c_L are nondimensional constants and ℓ is the spacing between binding sites. Then, plugging into Eq. (10) we find

$$f(x) = \lim_{\kappa\to\infty} f_0 \exp\left\{\left(-\frac{\kappa x^2}{2k_bT}\right) + \frac{c_w}{\ell}\left[\sqrt{\left(\frac{c_L k_b T}{\ell\kappa}\right)^2 + x^2} - \frac{c_L k_b T}{\ell\kappa}\right]\right\} \approx f_1 \delta(x),$$

where $f_1 \approx \lim_{\kappa\to\infty} f_0\sqrt{2\pi k_b T/\kappa}$ is a constant (note that, for finite f_1, we need $f_0 \to \infty$). Similarly, plugging into Eq. (11):

$$g(x) = \lim_{\kappa\to\infty} g_0 \exp\left\{\frac{c_w}{\ell}\left[\sqrt{\left(\frac{c_L k_b T}{\ell\kappa}\right)^2 + x^2} - \frac{c_L k_b T}{\ell\kappa}\right]\right\} \approx g_1 \exp(a|x|),$$

where $g_1 = g_0$ and $\alpha = c_w/\ell$ are constants. These simplifications apply for large b and small c.

In the following, we use the smooth rate functions Eqs. (10) and (11) for the numerical simulations, but use the simpler and less-smooth rate functions

$$f(x) = f_1\delta(x) \quad \text{and} \quad g(x) = g_1 e^{a|x|} \tag{12}$$

when attempting analytical approximations.

Both Eqs. (10) and (11) and the simplified expressions in Eq. (12) were derived assuming that the position of the binding site (x) could vary. In other words, these equations provide expressions for the *strain* dependence of rate constants. Previous researchers have derived expressions for the *load* dependence of rate constants by adding a linear function of x to a two-welled potential energy surface [43,60–65]. The load-dependent rate constants are similar but not equivalent to the strain-dependent rate constants. We discuss these differences in more detail in Sec. IV.

The mechanical model presented here for binding is not the only reasonable one (Fig. 3). Here, we have assumed ε_2 to be a spatial coordinate. Instead, one might consider ε_2 to be a generic reaction coordinate. This interpretation of ε_2 would allow us to move the position of the binding well B in a more general manner in the $\varepsilon_1 - \varepsilon_2$ plane, perhaps giving rise to slightly different rate functions.

Finally, the binding site model is nominally one dimensional (Fig. 1) and the rate functions were derived using a two-dimensional model (Fig. 3). However, we acknowledge that friction involves, in detail, the three-dimensional interaction between not-quite flat surfaces. But the simplifications here are natural and common in the friction literature.

III. PROPERTIES OF THE DENSE BINDING SITE MODEL

We obtain the response of the dense binding site (Lacker-Peskin) friction model under three different types of experiments. First, we derive analytic expressions for steady-state friction force at various slip velocities and then obtain simplified expressions for this force-velocity relation in various limits. Next, we perform numerical simulations of step changes in sliding velocity and the resulting transient response of our model. We argue that one expects a transient increase in friction force for step increases in slip velocity. Finally, we consider the classic "stick-slip" setup, in which there is a compliant element between the applied force and the sliding block. In these numerical simulations, we found stable sliding at low velocity; while at high velocity, we found both stable sliding and oscillatory slip depending on parameter values. Several of these trends and phenomena agree qualitatively with some friction experiments.

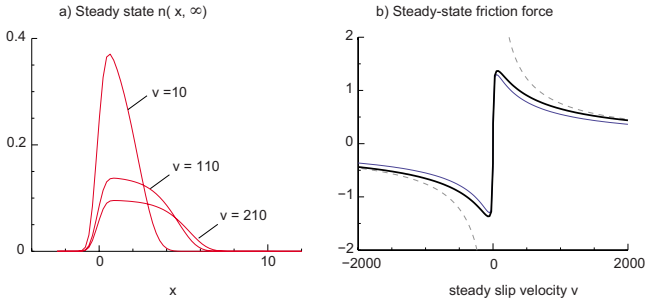

FIG. 4. (Color online) Steady slip for the Lacker-Peskin friction model. (a) The distribution of bound cross-bridges for three different slip velocities. (b) The steady-state friction force as a function of steady slip velocity. The solid dark line is the result of a numerical solution with smooth rate functions based on Eqs. (10) and (11). The thin solid line is the complete analytical solution [Eq. (19)] using simplified rate functions [Eq. (12)]. The dashed line is the large velocity approximation [Eq. (21)] to the analytical solution.

A. Steady slip

At zero slip velocity and steady state, one obtains the unique value for $n(x,\infty)$ to be

$$n(x,\infty) = \left(1 - \int_{-\infty}^{\infty} n dx\right)\frac{f_p(x)}{g_p(x)}, \tag{13}$$

an even function of x, implying zero net force. In this strict sense, this model exhibits no static friction for the f_p and g_p that we use. However, it is possible to construct $f_p(x)$ and $g_p(x)$ that do give rise to nonunique $n(x,t)$ at $v=0$ and, therefore, true static friction (see Appendix C).

For positive v, the cross-bridges get pulled into positive strains $x>0$, so that the steady state $n(x)$ is asymmetric about $x=0$. Figure 4(a) shows the asymmetric steady-state distributions $n(x)$ for a few different steady positive slip velocities, for the Lacker-Peskin model with smooth rate functions $f_p(x) = f(x)/h$ and $g_p(x) = g(x)$ from Eqs. (10) and (11), with $h=0.1$. Figure 4(b) shows the steady-state friction force as a function of slip velocity. We see that the friction force is zero for zero velocity, increases very rapidly to a finite force for small velocities, and then goes to zero as the velocity goes to infinity. The rapid increase in friction force for small velocities imply that in an experiment in which the external

force pulling the two surfaces apart is increased extremely slowly, the corresponding slip will be very small until a threshold force is reached. This behavior is reminiscent of static friction, even though this is not "true" static friction. (Indeed, when computational mechanicians wish to simulate Coulomb friction using smooth equations, they sometimes use functions such as $\tan^{-1}(v/\epsilon)$ that rapidly rises from zero for small v and then asymptotes to a constant. See, for instance, [66].)

Using the simplified rate functions of Eq. (12), it is possible to derive exact analytical expressions for the steady-state force-velocity relation. Using the simplified rate functions, the Lacker-Peskin PDE becomes

$$\frac{\partial n}{\partial t} + v\frac{\partial n}{\partial x} = (1-N)f_{1p}\delta(x) - ng_1 e^{a|x|}, \tag{14}$$

where $N(t)=\int_{-\infty}^{+\infty} n(x,t)dx$ is the fraction of all cross-bridges that are bound at time t, whatever their strain x. At steady state, $\partial n/\partial t=0$, so that

$$v\frac{dn}{dx} = (1-N)f_{1p}\delta(x) - ng_1 e^{a|x|}.$$

Because there are no attachments for $x<0$, $n(x<0)\equiv 0$. The large binding rate at $x=0$ produces a jump in $n(x)$ equal to $n(0^+)=(1-N)f_{1p}/v$. For $x>0$, the steady-state differential equation reduces to

$$v\frac{dn}{dx} = -g_1 n e^{ax}. \tag{15}$$

Solving for $n(x)$, we have

$$n(x) = n(0^+)e^{-B(e^{ax}-1)}, \tag{16}$$

where $B=g_1/av$, a convenient notation. So the total fraction bound, N, is given by

$$\begin{aligned} N &= \int_{0^+}^{\infty} n(x)dx \\ &= \frac{f_{1p}}{av}e^B(1-N)\int_{0^+}^{\infty} e^{-Be^X}dX \\ &= HB(1-N)E_1(B)e^B, \end{aligned} \tag{17}$$

where $X=ax$, $H=f_{1p}/g_1$, and $E_1(B)$ is the so-called exponential integral [67], a positive and monotonically decreasing nonelementary function defined for $B>0$. $E_1(B)$ goes to zero as B goes to infinity and goes to infinity as B approaches zero.

Solving Eq. (17) for N gives

$$N = \frac{HBE_1(B)}{HBE_1(B)+e^{-B}} \tag{18}$$

and then

$$n(x) = \frac{a}{E_1(B)+e^{-B}/HB}e^{-Be^{ax}}.$$

The total force F due to the ensemble of attached cross-bridges is given by

$$\begin{aligned} F &= M\int_{0^+}^{\infty}(\kappa x)n(x)dx = \frac{M\kappa n(0^+)e^B}{a^2}\int_{0^+}^{\infty} Xe^{-Be^X}dX \\ &= \frac{M\kappa}{a}\frac{Q(B)}{E_1(B)+e^{-B}/HB}, \end{aligned} \tag{19}$$

where

$$\begin{aligned} Q(B) = \int_0^{\infty} Xe^{-Be^X}dX &= \frac{\pi^2}{12} + \frac{\gamma^2}{2} + \gamma\ln B + \frac{(\ln B)^2}{2} \\ &\quad - BG([1,1,1],[2,2,2],-B), \end{aligned} \tag{20}$$

where G is the generalized hypergeometric function, also called the Barnes extended hypergeometric function [68]. Here, $\gamma\approx 0.577\,215\,6\ldots$ is the Euler-Mascheroni constant, not to be confused with the damping coefficient in the rate function derivation. Equation (19) is the thin dashed line in Fig. 4(b) and compares well with the numerical simulations (thick dashed line) with the smoother rate functions [Eq. (12)].

Equation (19) is amenable to further simplification, for which we define a nondimensional force $\bar{F}=aF/M\kappa$ per cross-bridge and a nondimensional velocity $V=1/B$. We consider two distinct cases below.

1. Finite attachment prefactor H

For large V and small B, noting that $Q(B)\sim 0.5(\ln B)^2$ and $E_1(B)\sim \ln B$, we have

$$\bar{F} = \frac{Q(B)}{E_1(B)+e^{-B}/HB} \approx 0.5H(\ln V)^2/V. \tag{21}$$

This expression makes it clear that the force goes to zero as the velocity goes to infinity, as V dominates $(\ln V)^2$. Equation (21) is the dashed line in Fig. 4(b). The large V approximation for finite H is applicable for "reasonable" velocities when H is small.

For sufficiently large B (and therefore, for small V), $E_1(B)=[1+\frac{1}{B}+O(\frac{1}{B^2})]e^{-B}/B$ [67]. So,

$$\begin{aligned} Q(B) &= \int_{0^+}^{\infty} E(Be^X)dX \\ &\approx \int_{0^+}^{\infty}\frac{e^{-Be^X}}{Be^X}dX \\ &= \int_1^{\infty}\frac{e^{-Bu}}{Bu^2}du \\ &= \frac{E_2(B)}{B} \\ &= \left[1+\frac{2}{B}+O\left(\frac{1}{B^2}\right)\right]\frac{e^{-B}}{B^2}, \end{aligned} \tag{22}$$

where $E_2(B)$ is the so-called exponential integral of order 2 (see [67]). Using these, we get

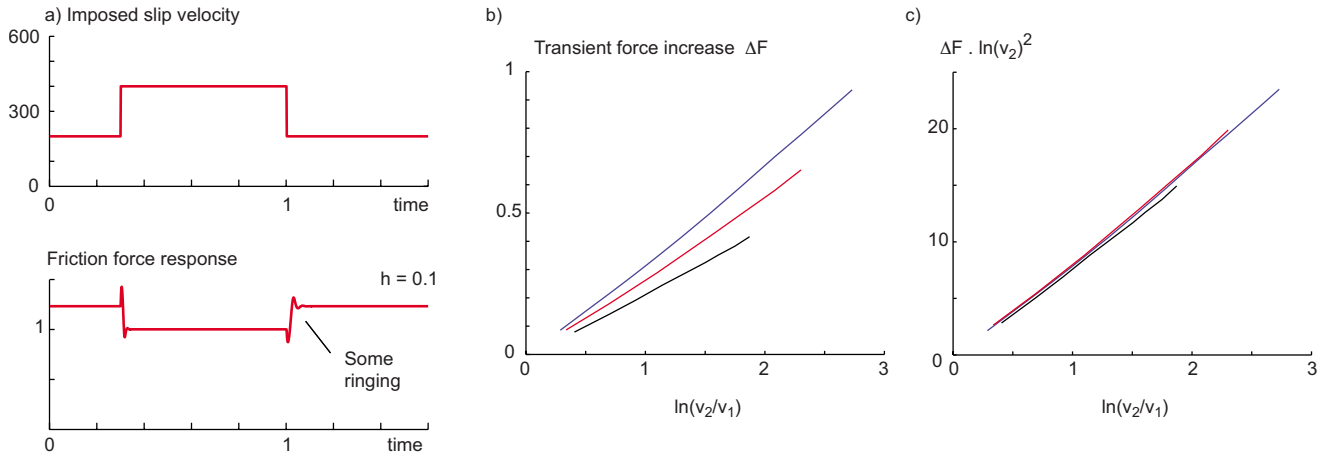

FIG. 5. (Color online) (a) Imposed step changes in slip velocity. (b) Force responses to step changes in slip velocity. A step up in velocity results in a transient increase in force but eventually converges to a lower steady-state force. This convergence, however, is oscillatory rather than monotonic. A step down in velocity results in the opposite behavior, but the transient decrease in force is smaller than the transient increase in force associated with a step up. Again, the convergence to the steady-state force is oscillatory. (c) Collapse of the different curves when plotted appropriately.

$$\bar{F} = \frac{Q(B)}{E_1(B) + e^{-B}/HB} \approx \frac{HV}{1+H}. \tag{23}$$

That is, the steady friction force increases linearly from zero at $v=0$ for small velocities.

Noting this increase at low velocities [Eq. (23)] and the decrease at higher velocities [Eq. (21)], we may infer that there is a maximum in between as seen in Fig. 4(b). This nonmonotonicity of the force-velocity relationship has been observed for elastomeric (rubber, polymeric) friction [28,43,69] for which closely related micromodels have been posited.

2. Infinite attachment prefactor H

The steady-state force-velocity relation for the Persson model [19] described in Appendix B may be obtained by taking the attachment prefactor f_1 and, therefore, $H=f_{1p}/g_1$ to infinity before obtaining the various velocity limits. A large H can result from either a large f_0 or a dense binding site limit, $h\to 0$. In this limit, the attachment is so strong that all the cross-bridges are always bound ($N\to 1$), albeit with different strains. This can be seen from Eq. (18) for N.

For $H\to\infty$, the force [Eq. (19)] simplifies to $\bar{F}=Q(B)/E_1(B)$. For sufficiently small B (and large $V>10$ say), $E_1(B)\approx -\gamma-\ln(B)$ and $Q(B)\approx \gamma\ln(B)+(\ln B)^2/2$, so that

$$\begin{aligned}\bar{F} &= \frac{\gamma\ln(B)+(\ln B)^2/2}{-\gamma-\ln(B)} \\ &= -\frac{\gamma+(\ln B)/2}{1+\gamma/\ln(B)} \\ &\approx -[\gamma+(\ln B)/2][1-\gamma/\ln(B)] \\ &\approx -\gamma/2+\frac{\ln V}{2}.\end{aligned} \tag{24}$$

We see that the friction force in this limit is simply proportional to $\ln V$. This logarithmic dependence of the friction force on velocity agrees with some friction experiments [38]. He and Robbins [12,13] performed molecular-dynamics simulations for adsorbed chain molecules caught between two atomically flat surfaces and they found a roughly linear increasing dependence between $\ln(V)$ and F for a few orders of velocity magnitude. Similarly, various instances of the Tomlinson model result in a logarithmic dependence of the force on the velocity [9,10,38]. This logarithmic dependence of force agrees with that obtained by Persson [19]. All this agreement is due to the similarity of the underlying physical assumptions in these various models.

For large B and small V, noting that $Q(B)\approx e^{-B}/B^2$ and $E_1(B)\approx e^{-B}/B$, we have

$$\bar{F} \approx \frac{1}{B} = V \text{ for small } V. \tag{25}$$

Thus, while the force-velocity relation for finite attachment prefactor is nonmonotonic, the force-velocity relation for the infinite attachment prefactor is monotonic increasing. Also, note that the limits $H\to\infty$ and $V\to\infty$ are not interchangeable here, since $e^{-B}/HB\approx V/H$ may or may not be negligible depending on how quickly V and H, respectively, approach infinity.

B. Transient force response to velocity changes

Measuring the response of the friction force to step changes in slip velocity has been a staple of rock-friction mechanicians [70–72] (but less common among those exploring friction at smaller scales) and provides important information about the stability of steady slip when the loading machine has some compliance (see Sec. III C). Of course, imposing step changes in velocity requires a sufficiently stiff loading machine, but can be done simply in theory here.

Figure 5 shows the transient friction force response of the Lacker-Peskin friction model to step changes in velocity. The

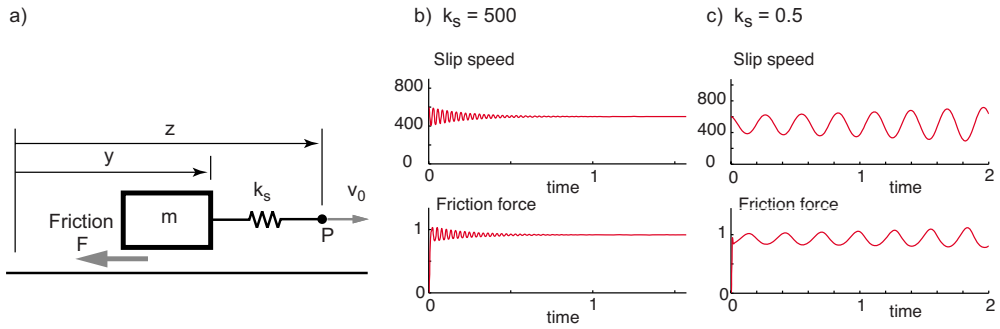

FIG. 6. (Color online) Stability of steady slip. (a) The mass m interacts with the surface through a Huxley friction model. The mass is dragged on the surface with a spring with stiffness k_s, with the force point P pulled at a constant velocity v_0. (b) Convergence to stable steady slip at $v_0=500$ with $m=0.001$, $k_s=500$, and $M=1$. (c) Oscillatory instability of steady slip at $v_0=500$ with $m=0.001$, $k_s=0.5$, and $M=1$.

friction force increases from the initial steady-state friction force F_1^{ss} at v_1 to a transient maximum $F_{\max}=F_1^{ss}+\Delta F_1$, before decaying to a final steady-state friction force F_2^{ss} corresponding to v_2. Physically, this transient increase in the force can be understood as the increased stretch of the already-attached cross-bridges, while the subsequent decrease in the force is due to a decrease in the fraction of attached cross-bridges.

Mathematically, if n_1 is the steady state n at v_1, when the velocity is suddenly changed from v_1 to v_2, the instantaneous rate of change of force is

$$\frac{dF}{dt} = M\int_{-\infty}^{\infty} (\kappa x)(\partial n/\partial t) \tag{26}$$

$$\sim (v_2 - v_1)\int_{-\infty}^{\infty} n_1(x)dx \tag{27}$$

using the fact that just after the transient, we have $\partial n/\partial t = (1-N_1)f_p(x) - n_1(x)g(x) - v_2\partial n_1/\partial x$, just before the transient, we have $0=(1-N_1)f_p(x)-n_1(x)g(x)-v_1\partial n_1/\partial x$, and then using integration by parts. The friction force here approaches the steady-state force in an oscillatory manner; note the slight undershoot below F_2^{ss} in Fig. 5(b) when the velocity was increased from v_1 to v_2.

Also, we find that the time scale over which the force attains steady state is inversely proportional to the new velocity (as can be noted from the PDE's) implying that there exists a characteristic distance over which such transients occur. Such a characteristic *distance* (as opposed to characteristic *time*) has been observed in analogous rock-friction experiments [70–72]. Finally, based on the physical mechanism for the transient force increase, it may be speculated that some other friction models with ensembles of springy elements might show such transient force increases

C. Stability of steady slip

When one body is dragged across another, with the two bodies interacting frictionally, a constant slip speed can be stable or unstable depending on the details of the frictional interactions and the loading paradigm. When steady slip is unstable, oscillatory slip—either smooth sinusoidal-like oscillations or relaxation oscillations—can be stable (sometimes called stick-slip [73,74]).

Consider first the situation in which the friction force is a simple point function of the slip velocity; that is, just a function of the instantaneous value of slip velocity with no dependence on its history or other state variables. Another common loading regime is shown in Fig. 6(a), in which the loading machine has compliance k_s and the point of force application P is moved at a constant velocity v_0. Again, if friction is a point function of slip velocity, a steady slip speed is stable if and only if the friction force is a locally increasing function of slip speed (The proof of these two slip stability results is elementary).

These conclusions are no longer necessarily true when the friction force ceases to be a point function of slip velocity. In the binding site friction models described here, the friction force is *not* a simple point function of slip velocity but instead depends on the detailed state of interacting surfaces as characterized by $n(x,t)$.

We performed numerical experiments with the Lacker-Peskin friction model to examine its response to the following: (1) a constant external force and (2) the loading setup shown in Fig. 6. For a given constant external force, two steady slip velocities are possible, as in Fig. 4, as long as the external force is not higher than the maximum friction force possible. We found, perhaps not surprisingly, that the lower equilibrium slip speed at which the steady friction force is an increasing function of slip speed is stable and the higher equilibrium slip speed is unstable.

The motion of the mass m in Fig. 6(a) is described by the equation

$$m\ddot{y} = k_s(z-y) - F, \tag{28}$$

where $z=v_0t$, $\dot{z}=v_0$, and F is the Lacker-Peskin friction force.

For low enough slip velocities, the steady-state friction force for the Lacker-Peskin model is an increasing function of slip velocity. When v_0 is in this range, we generally found that steady slip with $\dot{y}=\dot{z}=v_0$ is stable in our numerical simulations of Eq. (28).

For large enough slip velocities, the steady-state friction force for the Lacker-Peskin model is a decreasing function of the steady slip velocity. At these speeds, perhaps surprisingly, both stable and unstable steady slips were observed.

Figure 6(b) shows an example of an asymptotic approach to stable steady slip and Fig. 6(c) shows an example of divergence from steady slip—both at the same pull velocity v_0 at which the steady-state friction force decreases with increasing slip velocity.

How can stability at these speeds be understood? Even though the steady-state friction force decreases with slip velocity (negative "steady-state viscosity"), the friction force increases transiently when there is a transient increase in slip velocity as observed in Sec. III B. Thus, if the slip velocity is changing rapidly enough (which it would at high loading machine stiffness k_s), the accompanying transient friction force oscillations is sufficiently in-phase to stabilize steady slip.

Somewhat analogously, the state-variable friction laws due to Ruina [71] had negative steady-state viscosity and (true) positive instantaneous viscosity. For this friction model, Rice and Ruina [73] showed similar stable steady slip at sufficiently high stiffnesses, even though the steady-state force decreased with steady slip speed. See Sec. IV B.

Filippov *et al.* [7] noted that they were able to obtain stick-slip only in the presence of an age-dependent contact model. In contrast, we find that both steady slip and oscillatory slip can be stable without having to assume age-dependent contact.

IV. DISCUSSION

We have presented a mathematical formalism for a class of friction models that describe the behavior of two rigid surfaces interacting by the formation and rupture of molecular bonds. These friction models agree qualitatively with some friction experiments. This model predicts a transient response to step changes in sliding speed that is in qualitative agreement with measured force transients in some rock-friction experiments. Additionally, the model can exhibit both stable sliding and stick-slip, even when the steady-state friction force decreases with speed. We now focus on three specific aspects for further discussion.

First, as promised earlier, we discuss the distinction between strain-dependent rate functions used here and the load-dependent rate functions more common in the literature. Next, we discuss the relevance of our results in the context of some state-variable friction models. Then, we discuss the importance of a connection between friction mechanics and biology, and potential applications of our results in biology.

A. Force vs strain-dependent rate constants

While the load applied to a molecule and the strain experienced by that molecule are related (in our model they are related quite simply by $F=\kappa\varepsilon$), there are important differences between expressions for rate constants derived assuming a constant applied load and those derived assuming constant strain. These differences arise because the spring in Fig. 3 does not apply a constant load, and in particular applies a larger load on the bound state than on the transition or unbound state, as explained below.

Load-dependent rate constants may be derived in the following way. Consider a double-well potential in one dimension $V_{dw}(x)$. We then add a constant force field so that the total potential is $V=V_{dw}(x)-Fx$. Note that in writing this relationship, we assume that force is *constant* along the reaction coordinate. If we make the simplistic assumption that the relative position of the critical points of V, the unbound state $x=0$, the transition state $x=\delta_c$, and the bound state $x=\delta_B$ are independent of load, then the unbinding rate is [60]

$$k_u = k_u^0 \exp\left(\frac{F(\delta_B-\delta_c)}{k_bT}\right). \tag{29}$$

This expression is valid in the limit of small F [61,63,64]. Similarly, the binding rate is

$$k_b = k_b^0 \exp\left(\frac{-F\delta_c}{k_bT}\right). \tag{30}$$

Using the model in Fig. 3, we can write $\delta_c=\sqrt{x^2+L^2}-w$ and $\delta_B=\sqrt{x^2+L^2}$. However, it is unclear what value we should choose for F in Eqs. (29) and (30). For example, using $F=-\kappa\delta_B$ in Eq. (29), the average spring force at the bound state (e.g., [7]) yields incorrect expressions for strain-dependent unbinding rate k_u. In fact, in order to get the correct expressions for strain-dependent k_u and k_b (as derived in Sec. II B), we must use $F=\kappa(\delta_c+\delta_B)/2$ in Eq. (29), the average value of spring force along the reaction coordinate for an unbinding reaction, and $F=\kappa\delta_c/2$ in Eq. (30), the average value of spring force along the reaction coordinate for a binding reaction. Therefore, for these simplest approximations valid at small F, while it is possible to use the load-dependent equations to find the correct strain-dependent rate constants, one must be careful to choose appropriate force values, namely, the average spring force along the reaction coordinate.

In our derivation of the binding and unbinding rates as a function of strain, we assumed that the distance to the transition state w was independent of strain, as was the curvature of the potential energy surface at the bound, unbound, and transition states. We justify these expressions by their simplicity. However, if more exact expressions are required, we could write Taylor expansions in these variables to obtain a series of more exact expressions (see [64] for this procedure applied to the load dependence of rate constants). In general, there is no simple way to translate between higher-order approximations derived at variable force and strain. Therefore, in order to get a consistent picture for both binding and unbinding rates, it is more rational to derive our rate constants as a function of strain.

B. Relation to empirical state-variable friction laws

In the models of friction we have described in this paper, the friction force at any instant is a function of the internal state of the system characterized by the function $n(x,t)$ and the evolution of this "state function" is governed by various partial differential equations as discussed. Thus, we may term our friction model, a state-function model of friction, in analogy to the state-variable friction laws proposed by Ruina and Dieterich [71,72] in which the internal states of the sliding surfaces are characterized by one or more state variables having their own evolution equations.

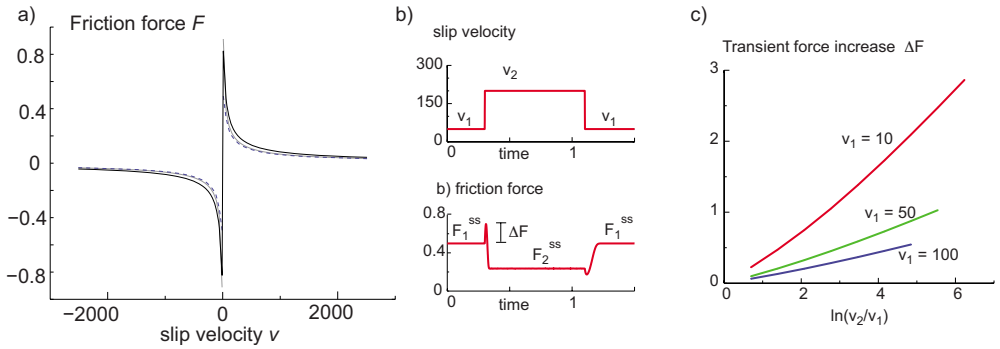

FIG. 7. (Color online) (a) Steady slip with the Huxley friction model. The friction force as a function of steady slip velocity. The solid black line is from numerical simulations of the Huxley model with $a=1$, $b=5$, $c=0.1$, $f_0=4$, $g_0=1$, and $\rho=1$. The solid gray line is the analytical solution assuming that the binding rate function is a Dirac delta function and the unbinding rate function is a simple increasing exponential [Eq. (A3)]. The dashed line is a large velocity approximation to the analytical solution [Eq. (A4)]. The solid gray line and the dashed line are essentially on top of each other on the scale of the plot. (b) Force responses to step changes in slip velocity. A step up in velocity results in a transient increase in force but eventually converges to a lower steady-state force. A step down in velocity results in the opposite behavior, but the transient decrease in force is smaller than the transient increase in force associated with a step up. (c) The transient increase in force as a function of the ln of the velocity change. The relation is close to linear especially for higher v_1.

The simplest such state-variable friction law, involving only one internal variable θ, that was found to agree with certain rock-friction experiments is the so-called Dieterich-Ruina equations introduced by Ruina [71] and closely related to that proposed by Dieterich [70]:

$$F = F_0 + \theta + a \ln\frac{v}{v_0}, \quad \dot{\theta} = -\frac{v}{d_c}\left(\theta + b \ln\frac{v}{v_0}\right). \tag{31}$$

Here, we briefly discuss the Dieterich-Ruina equations [Eq. (31)] in the context of results from our state-function models of friction. At steady slip v, Eq. (31) implies $\dot{\theta}(\infty)=0$, $\theta(\infty)=-b\ln(v/v_0)$, and the steady-state friction force is $F^{ss}=F_0+(a-b)\ln(v/v_0)$. Usually in experiments with macroscopic samples [71], it is found that $b>a$, so that the steady-state friction force F^{ss} is a decreasing function of velocity, as is the large velocity limit of both the Lacker-Peskin and Huxley friction models. (Note that these state-variable friction laws are not meant to be applicable for arbitrarily large velocities where the steady-state force at constant slip velocity erroneously evaluates to a negative quantity.)

Second, Eq. (31) implies a transient increase in force corresponding to a step increase in slip velocity. It is easy to see that $\Delta F=a\ln(v_2/v_1)$ is the instantaneous change in friction force associated with an instantaneous change in velocity from v_1 to v_2 (θ having no time to evolve). After this increase, the force slowly decays to a lower steady state F_2^{ss} at the higher velocity v_2. The property that there is a transient increase in the friction force, despite the steady-state force decreasing with slip speed, is qualitatively similar to that of both the friction models presented here.

The discontinuous step change in friction force in response to a step change in velocity is due to the explicit dependence of the friction force on the velocity v (in addition to the internal variable θ), when $a\neq 0$. This is perhaps a key difference between the state-variable friction laws of Ruina and Dieterich and our state-function models of friction. In our Huxley and Lacker-Peskin friction models, the friction force is not an explicit function of the slip velocity; so changes in velocity can affect the friction force only through changes in the state function $n(x,t)$, which can change only continuously.

Next, in the state-variable friction laws [Eq. (31)], and in the rock-friction experiments that motivated them, the ΔF appear to be simply proportional to $\ln(v_2/v_1)$. For both the Lacker-Peskin and Huxley models, it appears that while ΔF is proportional to $\ln(v_2/v_1)$ for a specific v_1, the proportionality constant is different for different v_1 [see Figs. 5(b) and 7(c)]. Finally, the Huxley model is perhaps closer qualitatively to the state-variable friction laws as the approach to steady state in the state-variable friction laws is nonoscillatory [Fig. 7(b)]. More generally, it seems likely that friction models presented here is more applicable directly for polymeric friction rather than rock friction.

C. Biological friction

Besides interest among the physics and mechanics community in deriving simple molecular models for friction, there is growing interest among the biological and biophysical community for such friction models. In many biological applications, aggregations of long-chain molecules (proteins) form and break molecular bonds between two surfaces that move relative to each other. For example, live cells growing on a surface form focal adhesions, local regions of the cellular membrane that bind to the surface. This binding occurs primarily through proteins called *integrins* anchored in the cell membrane that then bind to the extracellular matrix (i.e., the surface of a coverslip). Cells apply load to these focal adhesions, which in turn slide across the surface. Recently, a number of frictionlike models have been proposed for focal adhesion dynamics [42,75]. We believe the analysis presented and the simple analytic expressions developed here are naturally applicable for such biological friction. The parameters of these analytic expressions relate to measurable

properties of the long-chain molecules (i.e., unloaded attachment rate, unloaded detachment rate, and elasticity).

In the models here (especially Sec. II B), for simplicity, we used the high-damping limit of Kramers' theory to derive binding and unbinding rates, which may not be the most appropriate for molecular interactions between two dry surfaces. However, biological friction (for instance, between two cells, or a cell and a substrate) mostly occurs in solution, so the high-damping Kramers' theory limit is quite appropriate. We expect that our analytic expressions, particularly the small V limits, will be useful in the modeling of biological friction. Furthermore, for biological friction, the parameters of the model, such as binding and unbinding rate in the absence of load and protein elasticity, can be measured with biochemical or biophysical methods. So we expect that the assumptions of the friction models can be simply and directly tested in this context. Also, by pointing out the closeness between molecular muscle models and friction models, we hope to encourage a healthy exchange of ideas between these two usually vastly separated fields.

V. CONCLUSIONS AND FUTURE WORK

We have proposed a class of friction models, describing friction arising from the formation and rupture of molecular bonds, generalizing and providing a formalized setting for some prior friction models, and having a number of properties qualitatively similar to general friction phenomenology. In particular, we have introduced and used a relationship for how rate constants for the formation and rupture of molecular bonds should depend on molecular strain in a simple case, which improves upon the load-dependent rate dependence usually used in friction models. We have derived as a limiting case, the properties of the Persson friction model, which gives a monotonically increasing force-velocity relation. Away from this limiting case, our friction models are capable of a nonmonotonic increasing-decreasing force-velocity relation found in some frictional regimes, such as elastomeric. We obtained simple asymptotic expressions for force-velocity relations in all these model and velocity regimes. We examined the response of our friction models to sudden imposed slip velocity transients and obtained transient increases in friction force even though there is a decrease in the steady-state friction force, somewhat analogous to the experimental results of Ruina. Responses to such velocity transients appear to have not been studied and explained previously in the context of microscopic friction models. Such responses to velocity transients also provide insight into the stability or otherwise of steady slip in the presence of compliance in a constant-velocity loading machine—a common source of stick-slip oscillations.

Future work will address one of the following many gaps in our account of these models. The discussion of these models' relation to experimental data at various scales has largely been qualitative here. By small modifications to either the rate functions f and g or to the models' basic assumptions, we hope to obtain fits to data from friction experiments. An important open problem in friction mechanics is the derivation of empirically based state-variable friction laws (such as [71,72]) from a microscopic theory perhaps such as that described here. Toward this end, we propose to construct Burridge-Knopoff-like models [32,33,76] in which a sequence of rigid blocks attached to springs, with each rigid block interacting with the surface by a Huxley or a Lacker-Peskin model. For instance, such hybrid models may increase the spatial scale of the force transients in response to velocity transients in the experiments of [72].

The practical utility of a state-function model might be questioned, since simulation of such a model requires considerable computational expense. Therefore, for many applications, a state-variable model would be more useful than a state-function model, even if an appropriate state-function model is found. But it is possible to reduce state-function models to state-variable models using appropriate low-dimensional projections (e.g., [77]).

ACKNOWLEDGMENTS

M.S. was supported by NSF Grant No. EF-0425878 awarded to Philip Holmes (Princeton University). We thank Andy Ruina (Cornell University) for first noting the possible similarity muscle and friction micromodels, organizing an informal workshop on these topics and inspiring this manuscript. Thanks to Herbert Hui for kindly listening to some early ideas. Thanks also to our anonymous referees for many constructive comments that have improved this paper.

APPENDIX A: HUXLEY FRICTION MODEL PROPERTIES

In this appendix, we briefly describe the properties of the Huxley sparse binding site model for friction. We discuss the steady-state dependence of friction force on sliding velocity and response to slip velocity transients.

At zero slip velocity and steady state ($t \to \infty$), we get $n_h(x,\infty) = f(x)/[f(x)+g(x)]$—an even function, giving zero steady force at zero velocity. In this sense, the Huxley friction model here has no static friction (but see Appendix C). For $v > 0$, bound cross-bridges with negative strains x are constantly pulled to positive strains. This convective term in the PDE makes n_h asymmetric about $x=0$ giving nonzero frictional forces. The steady-state friction force as a function of steady slip velocities v is shown (black solid line) in Fig. 7(a). We see that the friction force for small velocities ($v > 0$) is nonzero rising very rapidly from zero force at zero slip speed. This high force for a range of very small velocities can be interpreted as being similar to static friction. The friction force decreases for higher velocities and approaches zero as $v \to \infty$. In this decreasing-force regime, the fraction of attached cross-bridges decreases; at such high velocities, the bound cross-bridges get pulled to higher strains quickly and therefore get unbound quickly.

Analytical approximations are obtained using simplified rate functions. Using these simplified rate functions $f(x) = f_1 \delta(x)$ and $g(x) = g_1 e^{a|x|}$ [Eq. (12)] in the steady-state Huxley PDE [Eq. (7)], we have

$$v \frac{dn_h}{dx} = (1 - n_h) f_1 \delta(x) - n_h g_1 e^{a|x|}. \tag{A1}$$

Solving this equation for $v > 0$, we obtain

$$n_h(x) = n_h(0^+)\exp[-B(e^{ax}-1)], \quad \text{for } x>0, \tag{A2}$$

and $n_h(x)=0$ for $x<0$, where $B=g_1/av$ and $n_h(0^+)=1-e^{-f_1/v}$. The total force F due to the ensemble of attached molecules is

$$F = n_h(0^+)\frac{\rho\kappa}{a^2}e^B Q(B), \tag{A3}$$

where $Q(B)$ is given by Eq. (20). This force-velocity relation is quite close to the force-velocity relation for the Huxley model with the smoother binding rate function [Eqs. (10) and (11)]. For small B, $Q(B)\approx\gamma\ln B+(\ln B)^2/2$ so that Eq. (A3) reduces to

$$F \approx (1-e^{-f_1/v})\frac{\rho\kappa}{a^2}\left[\gamma\ln B+\frac{1}{2}(\ln B)^2\right] \tag{A4}$$

shown as a dotted line in Fig. 7(a). Conversely, for large B and small v, $Q(B)$ goes to zero, as is consistent with the friction force vanishing at zero velocity.

Unlike the Lacker-Peskin model, the transients in friction force from the Huxley model, when subject to sudden slip velocity changes, do not show ringing. Figure 7(b) shows the response of the force from the Huxley friction model to step changes in the imposed slip velocity, from v_1 to v_2 and back. The friction force increases from the initial steady-state friction force F_1^{ss} at v_1 to a transient maximum $F_{\max}=F_1^{ss}+\Delta F_1$, before decaying to a final steady-state friction force F_2^{ss} corresponding to v_2. That is, though the steady-state friction is a decreasing function of the slip velocity (negative steady-state viscosity), the friction force increases in response to step increases in velocity (positive short-time-scale viscosity for velocity transients). Figure 7(c) shows the transient increase ΔF in the force as a function of $\ln(v_2/v_1)$ for three different v_1. We see that, for a given v_1, ΔF is close to proportional to $\ln(v_2/v_1)$, somewhat similar to the state-variable friction laws [72] as discussed in Sec. IV B. Finally we note that the Huxley friction model also rise to both stable steady slip and stable oscillatory slip based on the stiffness of the loading mechanism and the pulling speed.

APPENDIX B: BINDING IMMEDIATELY AFTER UNBINDING—THE PERSSON MODEL

Persson derives the following equation for his friction model, which is shown to be a special case of the Lacker-Peskin model:

$$\frac{\partial\eta}{\partial t}+\frac{k_1 v}{\delta A}\frac{\partial\eta}{\partial\sigma} = -g(\sigma)\eta + f(\sigma)\int_{-\infty}^{\infty} g(\sigma')\eta d\sigma',$$

where the stress σ is related to strain ε by $\sigma=\varepsilon k_1/\delta A$. Here k_1 is the spring constant and δA is the small area of a particular pinned region. For the detachment function $g(\sigma)$, he uses the following expression for $|\sigma|\le\sigma_a$:

$$g(\sigma) = \nu\exp[-\beta\Delta E(\sigma)] = \nu\exp(-\beta\epsilon[1-(\sigma/\sigma_a)^2]),$$

where $\beta=1/k_BT$ and $\nu=k_a/2\pi m\gamma$. He assumes that detachment is instant for $|\sigma|>\sigma_a$. The attachment function is a delta function: $f(\sigma)=\delta(\sigma)$.

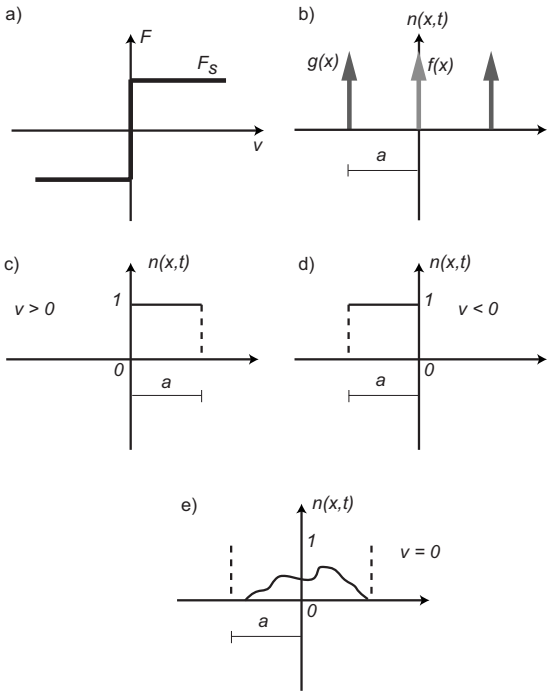

FIG. 8. Coulomb friction as a special case of the Huxley model. (a) The force-velocity relationship for Coulomb friction. (b) The binding and unbinding rate functions for the special-case Huxley model leading to Coulomb friction. The binding function is a Dirac delta function $f_0\delta(x)$ with $f_0\to\infty$. The unbinding function is a sum of two Dirac delta functions $g_0[\delta(x-a)+\delta(x+a)]$ with $g_0\to\infty$. (c) The steady state $n(x,t)$ for steady slip velocity $v>0$. (d) The steady state $n(x,t)$ for steady slip velocity $v<0$. (e) The steady state $n(x,t)$ is not unique for $v=0$. One such steady solution is shown. This nonuniqueness enables the friction force to be multiple valued at $v\equiv 0$.

It is not hard to see that the Persson model is a Lacker-Peskin model

$$\frac{\partial n}{\partial t}+v\frac{\partial n}{\partial\varepsilon} = -g(\varepsilon)n + f(\varepsilon)(1-N)$$

with the following attachment and detachment functions:

$$g(\varepsilon) = \begin{cases} g_0\exp[\beta\epsilon(\varepsilon/\varepsilon_a)^2]: & |\varepsilon|\le\varepsilon_a \\ \infty: & |\varepsilon|\ge\varepsilon_a \end{cases}$$

$$f(\varepsilon) = \lim_{f_0\to\infty}\frac{f_0 k_1}{\delta A}\delta(\varepsilon).$$

The assumption here is that attachment is instant and that attachment occurs at $\varepsilon=0$.

It may not be obvious that $f(\varepsilon)(1-N)$ is equal to the second term on the right-hand side of the Persson differential equation. To see this, we first observe that the total number of attached cross-bridges is constant in the Persson model (i.e., $\int_{-\infty}^{\infty}\eta(\sigma')d\sigma'=N_P$). Then, we use the steady-state version of Persson's differential equation to show that

$$N_P = \frac{\delta A}{k_1 v}\int_0^\infty g(\sigma')\,\eta d\sigma' \int_0^\infty \exp\left[-\frac{\delta A}{k_1 v}\int_0^\sigma g(\hat{\sigma})d\hat{\sigma}\right]d\sigma.$$

From the steady-state solution to the Lacker-Peskin equation, it can be shown that

$$1-N = \lim_{f_0\to\infty} \frac{1}{1+\frac{f_0}{v}\int_0^\infty \exp\left(-\int_0^\varepsilon \frac{g(\hat{\varepsilon})}{v}d\hat{\varepsilon}\right)d\varepsilon}.$$

Therefore,

$$1-N = \lim_{f_0\to\infty} \frac{1}{1+f_0\frac{N_P}{\int_0^\infty g(\sigma')\,\eta d\sigma'}}.$$

Then, the attachment rate $f(\varepsilon)(1-N)$ is

$$\lim_{f_0\to\infty} \frac{f_0\delta(\sigma)}{1+f_0\frac{N_P}{\int_0^\infty g(\sigma')\,\eta d\sigma'}} \approx \delta(\sigma)\frac{\int_0^\infty g(\sigma')\,\eta d\sigma'}{N_P}.$$

APPENDIX C: RATE-INDEPENDENT COULOMB FRICTION AS A SPECIAL CASE

With somewhat idealized rate functions $f(x)$ and $g(x)$, it is possible to make both the Huxley and the Lacker-Peskin models behave like rate-independent Coulomb friction [Fig. 8(a)], including *static friction*—that is, ability to resist a range of external forces at zero slip. We briefly describe a Huxley-like Coulomb-friction model below. The binding function is such that every cross-bridge gets bound when it crosses $x=0$ [that is, $f(x)=f_0\delta(x)$ with $f_0\to\infty$]. The unbinding function is such that every bound cross-bridge remains attached until a threshold strain a is reached, at which point every cross-bridge with that strain unbinds. No cross-bridge can have a strain $|x|>a$. For any $v>0$, the distribution $n(x,t)$ of cross-bridges converges to that shown in Fig. 8(c). The steady state $n(x,t)$ for negative v is shown in Fig. 8(d), giving a friction force equal to $-F(|v|)$, making the force-velocity relation an odd function.

At zero slip velocity ($v=0$), the steady state $n(x,t)$ is not unique. Any $n(x,t)$ such that $n(x,t)\le 1$ when $-a\le x\le a$ and $n(x,t)=0$ when $|x|>a$ is a steady solution. An example is shown in Fig. 8(e). This nonuniqueness in n corresponds to the nonuniqueness in the friction force at $v=0$ corresponding to genuine static friction. The necessary and sufficient condition for nonunique steady state n at $v=0$ is that there is a region (a,b) over which $f=g\equiv 0$. See [78,79] for an elaboration of these ideas.

More generally, the reader may observe that the steady-state forces are independent of the velocity if the rate functions are proportional to the velocity; that is, $f=vp(x)$ and $g=vq(x)$. Then, the Huxley PDE, for instance, at steady state reduces to $dn/dx=(1-n)p(x)-nq(x)$, an equation that has no dependence on the velocity (Ruina, personal communication). The Lacker-Peskin friction model with similar binding and unbinding functions behaves similarly to the Huxley Coulomb-friction model here.

[1] F. Al-Bender, V. Lampaert, and J. Swevers, Chaos **14**, 446 (2004).
[2] N. M. Beeler, T. E. Tullis, and D. L. Goldsby, J. Geophys. Res. **113**, B01401 (2008).
[3] O. M. Braun and M. Peyrard, Phys. Rev. Lett. **100**, 125501 (2008).
[4] R. J. Cannara, M. J. Brukman, K. Cimatu, A. V. Sumant, S. Baldelli, and R. W. Carpick, Science **318**, 780 (2007).
[5] M. Cieplak, E. D. Smith, and M. O. Robbins, Science **265**, 1209 (1994).
[6] C. Daly, J. Zhang, and J. B. Sokoloff, Phys. Rev. Lett. **90**, 246101 (2003).
[7] A. E. Filippov, J. Klafter, and M. Urbakh, Phys. Rev. Lett. **92**, 135503 (2004).
[8] A. E. Filippov and V. L. Popov, Phys. Rev. E **75**, 027103 (2007).
[9] C. Fusco and A. Fasolino, Phys. Rev. B **71**, 045413 (2005).
[10] E. Gnecco, R. Bennewitz, T. Gyalog, Ch. Loppacher, M. Bammerlin, E. Meyer, and H.-J. Güntherodt, Phys. Rev. Lett. **84**, 1172 (2000).
[11] G. He, M. H. Müser, and M. O. Robbins, Science **284**, 1650 (1999).
[12] G. He and M. O. Robbins, Tribol. Lett. **10**, 7 (2001).
[13] G. He and M. O. Robbins, Phys. Rev. B **64**, 035413 (2001).
[14] B. Luan and M. O. Robbins, Phys. Rev. E **74**, 026111 (2006).
[15] C. M. Mate, MRS Bull. **27**, 967 (2002).
[16] J. S. McFarlane and D. Tabor, Proc. R. Soc. London, Ser. A **202**, 244 (1950).
[17] D. Mulliah, S. D. Kenny, and R. Smith, Phys. Rev. B **69**, 205407 (2004).
[18] M. H. Müser, L. Wenning, and M. O. Robbins, Phys. Rev. Lett. **86**, 1295 (2001).
[19] B. N. J. Persson, Phys. Rev. B **51**, 13568 (1995).
[20] M. R. Sørensen, K. W. Jacobsen, and P. Stoltze, Phys. Rev. B **53**, 2101 (1996).
[21] J. Ringlein and M. O. Robbins, Am. J. Phys. **72**, 884 (2004).
[22] M. G. Rozman, M. Urbakh, and J. Klafter, Phys. Rev. Lett. **77**, 683 (1996).
[23] J. B. Sokoloff, Phys. Rev. B **65**, 115415 (2002).
[24] G. A. Tomlinson, Philos. Mag. **7**, 905 (1929).
[25] M. Weiss and F. J. Elmer, Phys. Rev. B **53**, 7539 (1996).
[26] M. Weiss and F. J. Elmer, Z. Phys. B **104**, 55 (1997).
[27] H. Yoshizawa, Y. L. Chen, and J. Israelachvili, Wear **168**, 161 (1993).
[28] Yu. B. Chernyak and A. I. Leonov, Wear **108**, 105 (1986).
[29] B. Bhushan, J. N. Israelachvili, and U. Landman, Nature (Lon-

don) **374**, 607 (1995)
[30] A. Ghatak, K. Vorvolakos, H. She, D. L. Malotky, and M. K. Chaudhury, J. Phys. Chem. B **104**, 4018 (1958).
[31] M. H. Müser, M. Urbakh, and M. O. Robbins, Adv. Chem. Phys. **126**, 187 (2003).
[32] J. M. Carlson and J. S. Langer, Phys. Rev. A **40**, 6470 (1989).
[33] J. M. Carlson and J. S. Langer, Phys. Rev. Lett. **62**, 2632 (1989).
[34] F. Horowitz and A. Ruina, J. Geophys. Res. **94**, 10279 (1989).
[35] Z. Olami, H. J. S. Feder, and K. Christensen, Phys. Rev. Lett. **68**, 1244 (1992).
[36] R. Burridge and L. Knopoff, Bull. Seismol. Soc. Am. **57**, 341 (1967).
[37] Z. Farkas, S. R. Dahmen, and D. E. Wolf, J. Stat. Mech.: Theory Exp. (2005), P06015.
[38] E. Gnecco, R. Bennewitz, T. Gyalog, and E. Meyer, J. Phys.: Condens. Matter **13**, R619 (2001).
[39] T. Gyalog, M. Bammerlin, R. Lüthi, E. Meyer, and H. Thomas, Europhys. Lett. **31**, 269 (1995).
[40] T. Gyalog and H. Thomas, Europhys. Lett. **37**, 195 (1997).
[41] D. Tománek, W. Zhong, and H. Thomas, Europhys. Lett. **15**, 887 (1991).
[42] A. Nicolas, B. Geiger, and S. A. Safran, Proc. Natl. Acad. Sci. U.S.A. **101**, 12520 (2004).
[43] A. Schallamach, Wear **6**, 375 (1963).
[44] T. L. Hill, Prog. Biophys. Mol. Biol. **28**, 267 (1974).
[45] T. L. Hill, Prog. Biophys. Mol. Biol. **29**, 105 (1975).
[46] F. C. Hoppensteadt and C. S. Peskin, *Mathematics in Medicine and the Life Sciences* (Springer-Verlag, New York, 1992).
[47] A. F. Huxley, Prog. Biophys. Biophys. Chem. **7**, 255 (1957).
[48] J. Keener and J. Sneyd, *Mathematical Physiology* (Springer-Verlag, New York, 1998).
[49] H. M. Lacker, Ph.D. thesis, New York University, 1977.
[50] H. M. Lacker and C. S. Peskin, *Lect. Math Life Sci.* (American Mathematical Society, Providence, RI, 1986), Vol. 16, pg. 121.
[51] C. S. Peskin, *Lectures on Mathematical Aspects of Physiology* (Courant Institute of Mathematical Sciences, New York, 1975).
[52] C. S. Peskin, *Mathematical Aspects of Heart Physiology* (Courant Institute of Mathematical Sciences, New York, 1975).
[53] A. F. Huxley and R. Niedergerke, Nature (London) **173**, 971 (1954).
[54] H. E. Huxley and J. Hanson, Nature (London) **173**, 973 (1954).
[55] Note that by adding multiple bound states with different strain-dependent detachment rates, it is possible to obtain a model with apparent "age-dependent" kinetics as proposed by [7].
[56] S. Walcott and S. X. Sun, Phys. Chem. Chem. Phys. **11**, 4871 (2009).
[57] J. S. Langer, Ann. Phys. **54**, 258 (1969).
[58] H. A. Kramers, Physica **7**, 284 (1940).
[59] W. Coffey, Y. P. Kalmykov, and J. T. Waldron, *The Langevin Equation: With Applications to Stochastic Problems in Physics, Chemistry and Electrical Engineering* (World Scientific, Singapore, 2004).
[60] G. I. Bell, Science **200**, 618 (1978).
[61] O. K. Dudko, A. E. Filippov, J. Klafter, and M. Urbakh, Proc. Natl. Acad. Sci. U.S.A. **100**, 11378 (2003).
[62] O. K. Dudko, G. Hummer, and A. Szabo, Phys. Rev. Lett. **96**, 108101 (2006).
[63] E. Evans, Annu. Rev. Biophys. Biomol. Struct. **30**, 105 (2001).
[64] S. Walcott, J. Chem. Phys. **128**, 215101 (2008).
[65] S. N. Zhurkov, Int. J. Fract. **1**, 311 (1965).
[66] S. J. Cull and R. W. Tucker, J. Phys. A **32**, 2103 (1999).
[67] M. Abramowitz and I. A. Stegun, *Handbook of Mathematical Functions with Formulas, Graphs, and Mathematical Tables* (Dover, New York, 1972).
[68] See documentation for MATLAB's HYPERGEOM function (The MathWorks, Inc.).
[69] K. A. Grosch, Proc. R. Soc. London, Ser. A **274**, 21 (1963).
[70] J. H. Dieterich, J. Geophys. Res. **84**, 2169 (1979).
[71] A. Ruina, Ph.D. thesis, Brown University, 1981.
[72] A. Ruina, J. Geophys. Res. **88**, 10359 (1983).
[73] J. R. Rice and A. L. Ruina, ASME J. Appl. Mech. **50**, 343 (1983).
[74] E. Rabinowicz, Proc. Phys. Soc. London **71**, 668 (1958).
[75] A. Besser and S. A. Safran, Biophys. J. **90**, 3469 (2006).
[76] J. M. Carlson, J. S. Langer, and B. E. Shaw, Rev. Mod. Phys. **66**, 657 (1994).
[77] G. I. Zahalak, Math. Biosci. **55**, 89 (1981).
[78] S. Walcott, Ph.D. thesis, Cornell University, 2006.
[79] S. Walcott and W. Herzog, Math. Biosci. **216**, 172 (2008).